

# Design of a Compact Millimeter Wave Antenna for 5G Applications based on Meta Surface Luneburg Lens

**Karedla Chitambara Rao**

Department of ECE, Aditya Institute of Technology and Management, Srikakulam, India  
rao.chiddubabu@gmail.com

**Dasari Nataraj**

Department of ECE, Swarnandhra College of Engineering and Technology, Narsapur, India  
dasari.nataraj@gmail.com (corresponding author)

**K. S. Chakradhar**

Department of ECE, Mohan Babu University, Tirupati, India  
chakradharec@gmail.com

**G. Vinutna Ujwala**

Department of ECE, St. Martin's Engineering College, Secunderabad, India  
ujwala459@gmail.com

**M. Lakshmunaidu**

Department of ECE, Koneru Lakshmaiah Education Foundation, Vijayawada, India  
laxman.naidu@gmail.com

**Harihara Santosh Dadi**

Department of ECE, Aditya Institute of Technology and Management, Srikakulam, India  
dhhsantosh@gmail.com

Received: 20 October 2024 | Revised: 1 December 2024 | Accepted: 12 December 2024

Licensed under a CC-BY 4.0 license | Copyright (c) by the authors | DOI: <https://doi.org/10.48084/etasr.9349>

## ABSTRACT

As the demand for fast and reliable wireless connectivity increases, the 5G technology has emerged as a promising solution. This study focuses on enhancing the gain and return loss performance of 5G wireless communication systems, with a particular emphasis on the Meta Surface Luneburg technique. In this work, a compact millimeter-wave antenna operating at a frequency of 28GHz dedicated to 5G applications is proposed and designed. The introduced design utilizes a metasurface Luneburg technique in order to obtain reduced size, high gain, and less return loss. The proposed antenna is implemented on a  $40 \times 40 \times 0.5 \text{ mm}^3$  RT Duroid 5880 Lossy substrate with a relative dielectric constant of  $\epsilon_r = 2.2$  and a loss tangent of 0.0068. Two-unit cells are strategically arranged in an array on the substrate to form a Luneburg meta-lens, which transforms spherical wavefronts into planar wavefronts. This configuration enables the antenna to achieve a directed beam at 28 GHz. The antenna is simulated, and key parameters, such as gain and return loss are analyzed. The results show that the antenna achieves a gain of 7.9 dBi and a return loss of less than -10 dB, demonstrating its suitability for 5G applications.

*Keywords-rectangular patch antenna; Luneburg lens technique; quarter-wave transformer; unit cells; frequency-selective surface*

## I. INTRODUCTION

The efficiency with which an antenna directs the power received from the transmitter towards a target is known as the antenna gain. The antenna gain can be increased by using larger antennas that capture more radio waves. Various antenna surfaces and shapes, along with gain enhancement techniques, such as metamaterial superstates, are employed to reduce reflection and substrate losses.

Modern wireless communication systems are actively investigating 5G frequencies because they offer fast data speeds and a vast amount of bandwidth to meet the demand for high volumes of data traffic and to make up for the scarcity of unlicensed frequency spectrum in the existing frequency bands [1]. The millimeter-wave range offers low latency, higher speeds, and greater bandwidth, making it essential for applications requiring high-gain wideband antennas. For 5G antennas, high gain, stable radiation patterns, and improved data handling are critical to achieve better coverage, reduced interference, and greater data throughput [2]. However, the structures, foliage, and precipitation can significantly absorb millimeter wavelengths sent at cellular network power levels. As a result, millimeter-wavelength communications are restricted to straight shot, requiring tiny cell networks that may raise the likelihood of edge interference amongst cells. To address these challenges, 5G antennas require beam-forming and high directivity capabilities to minimize disruption and maximize range by concentrating beam energy. As small cell deployments become more common, compact antenna designs suitable for installation on light poles and building corners are increasingly critical. To reimburse for various losses, millimeter-wave applications need high gain of antennas due to the significant atmosphere attenuation and the limited yield power of millimeter-wave solid-state sources [3]. Owing to the ohmic loss and surface waves, Microstrip Antennas (MSAs) have a low intrinsic gain at 5G frequencies. Both longer transmission distances and lower transmitter power consumption result from improving an antenna's gain.

Several methods for improving the gain of MSAs have been put forth recently. Gain enhancement techniques have been used to H-shaped resonator structures [4] and hybrid substrates [5] with ferrite rings implanted in them. A several number of split-ring resonator unit cells are arranged in an array and then integrated for increasing the gain into the orthogonal plane [6]. For gain augmentation, the MSA can be merged with a cylindrical electromagnetic bandgap substrate or a single-layer Eddy electric substrate embedded with holes of different diameters. Dielectric lenses have a high profile, which makes them heavy [7, 8]. The high electrical thickness lens's dielectric constant can be altered by changing its curvature and, consequently, its configuration, which promotes phase aggregation. As reflectors beneath MSAs, Frequency-Selective Surfaces (FSS) [9-12] have been used to increase gain. The simplicity of manufacture, small size, and lower insertion losses of meta surfaces when compared to three-dimensional structures have made them quite popular in recent years. When electric and magnetic fields are incident on them, they help to systematically manipulate their spatial distributions. The unit cells that comprise the lens's geometry determine whether the

electromagnetic waves that impinge on the meta surfaces are reflected or transmitted. For obtaining high-gain antennas, the planar lens is an excellent option due to its many advantages, such as its lightweight design, smooth surface, large gain, ease of manufacturing, and basic feeding mechanism. The focusing or collimating characteristics of the lens have led to the employment of lens antennas [13-15] for both transmission and reception. For communications using short wavelengths, they are by far the most favoured candidates. Due to the large insertion loss in higher frequency bands, multilayer metamaterial setups significantly diminish the effectiveness of the antenna's radiation [16, 17]. At 0.10 GHz, a low-profile lens antenna has been envisioned using a Graded Index Meta Surface (GIMS) lens vertically mounted on top of a microstrip patch antenna for greatest gain [18]. Even though a mushroom-shaped dielectric lens has been occupied to improve the opposite planar log-periodic dipole antenna's stable gain, its deployment is significantly hampered by the complex production process [19]. For the purpose of enhancing the gain of a dual-fed linearly polarised patch antenna, a microwave lens made of thirteen periodic dielectric sheets is proposed; however, due to its larger profile, it is not appropriate for 5G applications that have limited space [20]. A parasitic lens that makes up the substrate has been employed to boost the gain of a patch antenna with reduced dimensions [21]. A fish-eye based half Maxwell lens has been fabricated using fractal metamaterial components to boost the gain of a monopole antenna [22]. The Vivaldi antenna's gain is enhanced when it is established close to the central point of a phase gradient meta surface with a four-split ring configuration [23]. Cost-effectively, a phase-graded index lens of 50 mm × 50 mm × 20 mm has been utilized to enhance the gain at 28 GHz [24]. A small, two-port, funnel-shaped MIMO antenna was created, modeled, built, and tested. The bandwidth varied from 23.6 to 26.3 GHz, the isolation was over 18 dB, the maximum obtained gain was 9.26 dB, and the return loss was 22 dB [25]. In this context, many researchers have explored gain enhancement strategies, such as phase gradient metasurfaces, H-shaped resonators, multilayered split-ring resonators, FSS, double-ring element-based lenses, and parasitic lens superstrates. This study presents a novel design for a Luneburg lens based on metasurface unit cells. A metasurface is an advanced extension of FSS with enhanced functionality. While the primary objective of an FSS is frequency filtering, achieved by inducing either an electric or magnetic response, it typically exerts limited control over the propagation of electromagnetic waves. Instead, it focuses on the transmission and reflection properties of the waves. In contrast, a metasurface stimulates both electric and magnetic responses, enabling greater control over electromagnetic wave propagation. This enhanced capability allows for the precise manipulation of wavefronts, including controlled refraction and reflection. The proposed structure operates as a metasurface lens, focusing electromagnetic waves to enhance the antenna's gain. The Luneburg lens is specifically designed to gather, concentrate, and direct electromagnetic waves to a targeted location. Constructed from a dielectric material with a variable refractive index, it can effectively focus and bend electromagnetic waves. A Luneburg lens is a gradient-index lens with spherical symmetry, where the refractive index decreases radially from its maximum at the

center to a minimum near the edges. This radial variation in the refractive index causes electromagnetic waves to bend and focus differently, allowing for a high gain and precise beam direction.

## II. ANTENNA DESIGN AND RESULTS

A compact millimeter-wave antenna with a Luneburg lens has been designed using two distinct unit cell architectures based on the FSS. These unit cells are engineered to exhibit a linearly varying transmission phase across the frequency range of 25 GHz to 35 GHz, ensuring gradual and controlled phase shifts. At the operating frequency of 28 GHz, the unit cells demonstrate selective band-pass filtering characteristics, allowing only the desired frequency components to pass through while reducing the unwanted transmissions. Additionally, the unit cells act as spatial filters and phase shifters enabling a 90° phase shift with an insertion loss of 3 dB. The design of each unit cell is optimized to achieve specific reflection and transmission properties at 28 GHz, contributing to the desired focusing and beam-directing characteristics of the Luneburg lens. By using a single layer metasurface structure, the unit cells ensure an efficient manipulation of the electromagnetic waves with minimal complexity. This approach enhances the overall antenna performance by leveraging the phase-shifting and filtering capabilities of the metasurface, achieving high gain and improved directivity.

### A. Design Equations

The design of the rectangular microstrip patch antenna is based on the following equations:

- Width of the patch:

$$W = \frac{v_o}{2f_r} \sqrt{\frac{2}{\epsilon_r + 1}} \quad (1)$$

- Length of the patch:

$$L = \frac{v_o}{2f_r \sqrt{\epsilon_{reff}}} \quad (2)$$

- Effective dielectric constant:

$$\epsilon_{reff} = \frac{\epsilon_r + 1}{2} + \frac{\epsilon_r - 1}{2} \left( \frac{1}{\sqrt{1 + \frac{2h}{W}}} \right) \quad (3)$$

- Extensive length:

$$\Delta L = 0.412h \frac{(\epsilon_{reff} + 0.3) \left( \frac{W}{h} + 0.264 \right)}{(\epsilon_{reff} - 0.258) \left( \frac{W}{h} + 0.8 \right)} \quad (4)$$

- Length of the ground:

$$L_g = 6h + L \quad (5)$$

- Width of the ground:

$$W_g = 6h + W \quad (6)$$

### B. Design Parameters

The proposed antenna is meticulously designed based on established design equations and principles to achieve optimal performance at the operating frequency of 28 GHz. The key

design parameters include the dimensions of the patch antenna, ground plane, substrate material, and the Luneburg lens unit cells. These parameters are carefully selected to ensure high gain, efficient beam direction, and effective operation in the millimeter-wave frequency range. The design parameters are summarized in Table I.

TABLE I. DESING PARAMETERS

	Parameter	Value
1	Resonant frequency ( $f_r$ )	28 GHz
2	Length of the patch ( $L$ )	3.29 mm
3	Width of the patch ( $W$ )	4.23 mm
4	Length of the ground ( $L_g$ )	6.29 mm
5	Width of the ground ( $W_g$ )	7.23 mm
6	Height of the substrate ( $h$ )	0.5 mm
7	Substrate dielectric constant ( $\epsilon_r$ )	2.2
8	Loss tangent ( $L_r$ )	0.0068
9	Wavelength ( $\lambda$ )	0.01 m

### C. Design Steps

The compact millimeter-wave antenna using the Luneburg lens was designed following a series of steps, with the corresponding return loss ( $S_{11}$ ) values having been assessed at each stage.

- **Step 1:** Patch antenna design without slot.

The initial design consists of a rectangular microstrip patch antenna without slots, with the following dimensions: patch length 3.29 mm, patch width 4.23 mm, length of ground plane 6.29 mm, and width of ground 7.23 mm, as can be seen in Figure 1. The antenna is fed by a quarter-wave transformer and is designed to resonate at a frequency of 28 GHz.

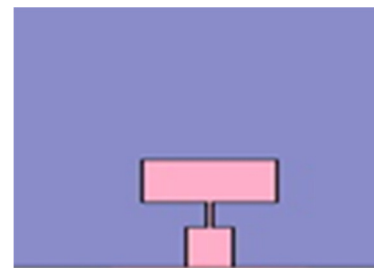


Fig. 1. Patch antenna without slot.

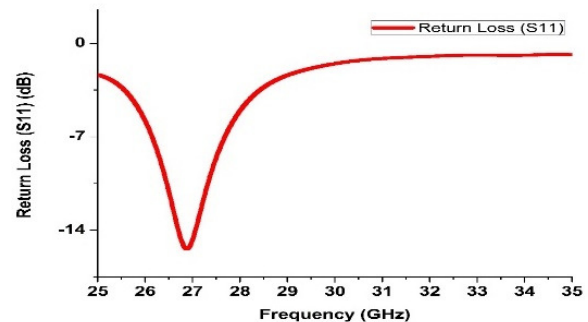


Fig. 2. Return loss ( $S_{11}$ ) of the microstrip patch antenna without slots.

The return loss ( $S_{11}$ ) of the initial antenna design was measured, revealing a value of less than -10 dB at 27 GHz rather than the intended operating frequency (28 GHz), as displayed in Figure 2. To achieve the desired resonance frequency of 28 GHz with a return loss of less than -10 dB, modifications were made to the design by introducing slots at the edges of the patch (Step 2).

• **Step 2:** Patch antenna design with slots.

To enhance the performance of the rectangular microstrip patch antenna, edge slots were introduced to fine-tune its operating characteristics, as depicted in Figure 3. These slots, with dimensions of 1 mm length and 1 mm width were strategically added to the antenna edges to improve resonance and gain at 28 GHz. The design parameters for the slotted antenna were carefully defined as:

$$\begin{aligned} x_{min} &= -0.25 \text{ mm}, & x_{max} &= 0.25 \text{ mm}, \\ y_{min} &= 1 \text{ mm}, & y_{max} &= -1.645 \text{ mm}, \\ z_{min} &= 0 \text{ mm}, & z_{max} &= 0.035 \text{ mm}. \end{aligned}$$

The introduction of these slots resulted in a realized gain of 4.9 dBi at the target frequency of 28 GHz, as portrayed in Figure 4. Although this represents an improvement, the gain remains insufficient to meet the high requirements for 5G applications. Integrating the antenna with a Luneburg lens presents a promising approach to address this limitation and achieve the desired performance. In terms of return loss ( $S_{11}$ ), the slotted design demonstrates a value of less than -10 dB at 28 GHz, confirming its effectiveness for wireless communication applications. Figure 5 illustrates the effect of return loss ( $S_{11}$ ) with different values of frequency.

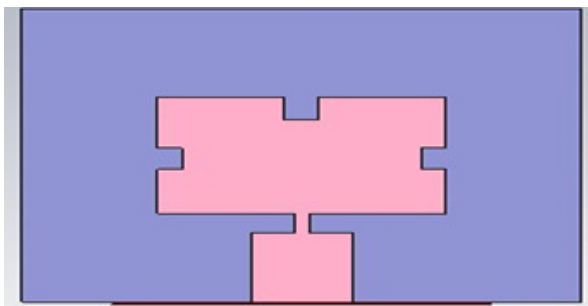


Fig. 3. Patch antenna with slots.

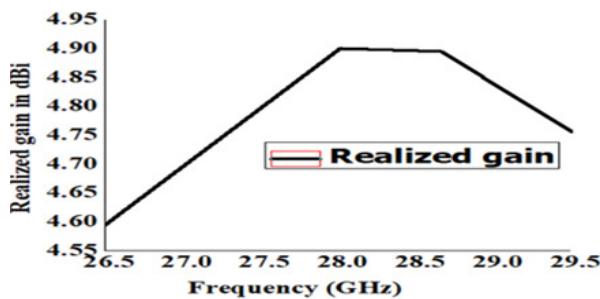


Fig. 4. The gain of the slotted antenna.

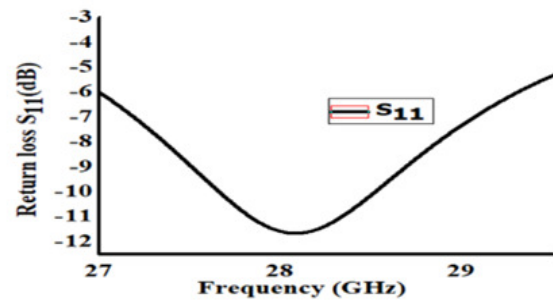


Fig. 5. The return loss ( $S_{11}$ ) of the slotted antenna.

• **Step 3:** Design of first unit cell.

The design of the first unit cell involves a combination of two circular rings and two overlapping four-legged loaded lenses, which resemble a pair of plus-sign-shaped structures. The circular rings are designated as the inner ring (ring 1) and the outer ring (ring 2). The inner ring has an inner radius of 3.6 mm and an outer radius of 4 mm, while the outer ring is designed with an inner radius of 4 mm and an outer radius of 8 mm. The four-legged loaded lenses, referred to as plus1 and plus2, are arranged such that one overlaps the other. The dimensions of plus1 are specified as 2.7 mm for the horizontal length and 2 mm for the vertical length. Similarly, plus2 has a horizontal length of 3.6 mm and a vertical length of 2.9 mm. The difference between the horizontal and vertical dimensions of the two plus-sign-shaped lenses is 0.9 mm. Once the two lenses are designed, they are positioned within the two circular rings, forming the complete structure of the first unit cell, as demonstrated in Figure 6.

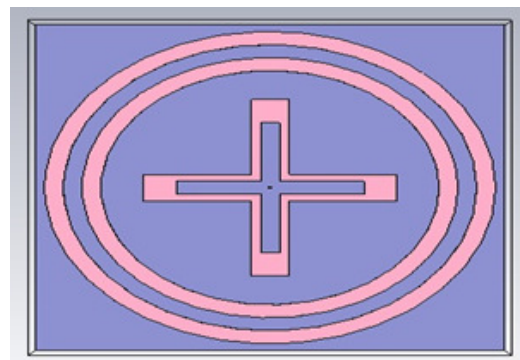


Fig. 6. Design of unit cell 1 consisting of two circular rings and two overlapping four-legged loaded lenses.

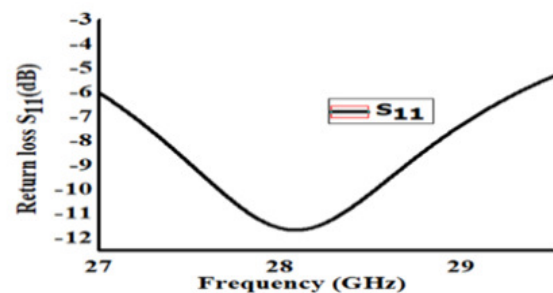


Fig. 7. Return loss ( $S_{11}$ ) of the first unit cell.

This intricate arrangement is crucial for achieving the desired electromagnetic performance. The return loss ( $S_{11}$ ) of this unit cell was also evaluated, as evidenced in Figure 7, with the results demonstrating that values below -10 dB are achieved at the operating frequency of 28 GHz.

• **Step 4:** Design of second unit cell

In the fourth stage, the second unit cell was developed using two plus-shaped lenses, as observed in Figure 8.

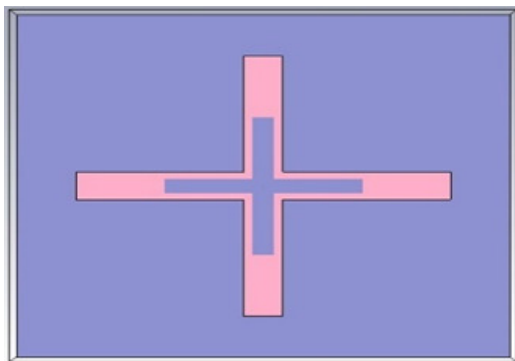


Fig. 8. Design of unit cell 2.

The top lens, referred to as Plus1, was designed with dimensions of 2.7 mm for the horizontal length and 2 mm for the vertical length. Similarly, the bottom lens, referred to as Plus2, was designed with horizontal and vertical lengths of 3.6 mm and 2.9 mm, respectively. This design emphasizes the structural variation between the two lenses, with the top and bottom elements complementing each other to achieve the desired electromagnetic properties for effective operation. The return loss ( $S_{11}$ ) for this unit cell shows acceptable values at the target frequency of 28 GHz, confirming the design's effectiveness, as showcased in Figure 9.

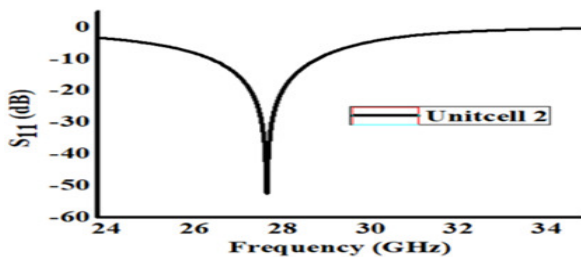


Fig. 9. Return loss ( $S_{11}$ ) of the second unit cell.

• **Step 5:** Design of frequency selective surfaces

The fifth step involves the development of an FSS on an RT Duroid 5880 lossy substrate. The substrate has dimensions of  $40 \times 40 \times 0.5 \text{ mm}^3$ , with a relative dielectric constant of  $\epsilon_r = 2.2$  and a loss tangent of 0.0068. Copper is utilized as a patch material due to its excellent conductive properties. The design features two circular rings:

1. Ring 1: This outer ring has an outer diameter of 40 mm and an inner diameter of 28 mm.

2. Ring 2: This inner ring has an outer diameter of 16 mm and an inner diameter of 4 mm.

Once the two circular rings are created, two-unit cells are arranged in an array on the FSS, as manifested in Figure 10. This configuration transforms the spherical wavefronts into planar wavefronts, creating a directed beam at the operational frequency of 28 GHz. This arrangement enhances the electromagnetic performance of the system by focusing the beam, making it suitable for high-gain applications, like 5G.

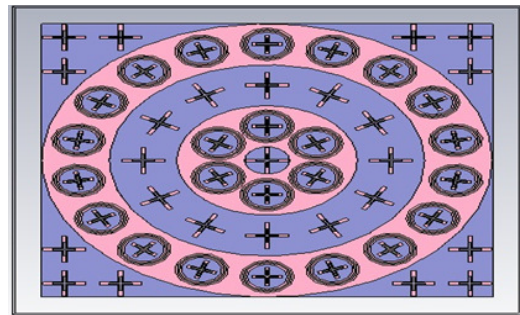


Fig. 10. FSS design.

• **Step 6:** Proposed antenna design

The proposed antenna design incorporates a slotted rectangular patch antenna with an array of two distinct unit cells, unit cell 1 and unit cell 2. These unit cells are arranged in a specific pattern to enhance the antenna's performance and create a directed beam at the target frequency of 28 GHz.

The design configuration includes: three-unit cells of unit cell 2) positioned at each edge of the substrate, eighteen-unit cells of unit cell 1 were arranged within ring 1 and six-unit cells of unit cell 1 were located in the small circle at the center. Moreover, twelve-unit cells of unit cell 2 were positioned in the space between the two circular rings. The front view of the design of the proposed antenna is illustrated in Figure 11, while the back view in Figure 12. This intricate arrangement of unit cells is critical for transforming spherical wavefronts into planar wavefronts, thereby directing the electromagnetic beam effectively. By leveraging the complementary properties of unit cell 1 and unit cell 2, the antenna achieves enhanced gain and beam focusing, making it highly suitable for millimeter-wave applications, such as 5G networks.

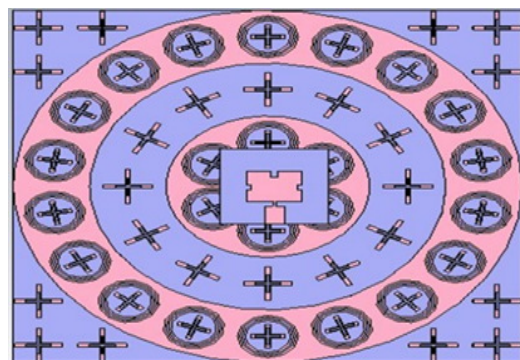


Fig. 11. Front view of the proposed antenna design.

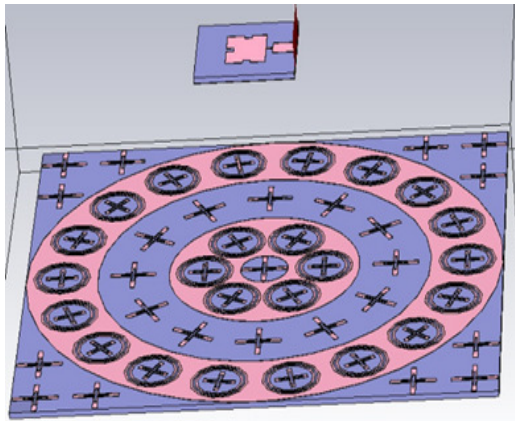


Fig. 12. Back view of the proposed antenna design.

The performance of the proposed antenna was evaluated in terms of its realized gain and return loss ( $S_{11}$ ), both of which meet the requirements for 5G applications at a frequency of 28 GHz. Specifically, the actual gain of the antenna was 7.9 dBi, as depicted in Figure 13. This gain is considered adequate for millimeter-wave 5G applications, ensuring reliable signal transmission and reception. The integration of the lens plays a significant role in achieving this gain enhancement. As for the return loss ( $S_{11}$ ) curve shown in Figure 14, it is indicated that the  $S_{11}$  parameter is -18 dB at 28 GHz. Since the value of  $S_{11}$  is less than -10 dB, it is deemed suitable for 5G applications. This ensures minimal signal reflection and efficient power transfer. Additionally, a comparison between the antenna's realized gain is being considered, with and without lens, as exhibited in Figure 15. With the lens, the realized gain reaches 7.9 dBi while without lens the realized gain is 4.9 dBi. This comparison highlights that the inclusion of the lens significantly enhances the gain, boosting it by 3 dBi. This gain improvement underscores the importance of the lens in achieving the desired performance metrics for advanced wireless communication systems.

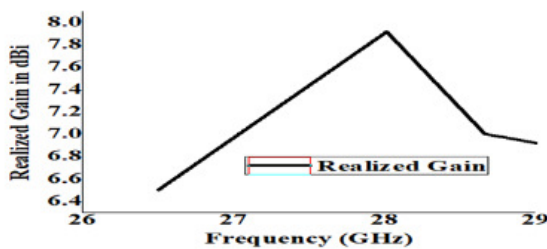


Fig. 13. Realized gain of the proposed antenna design.

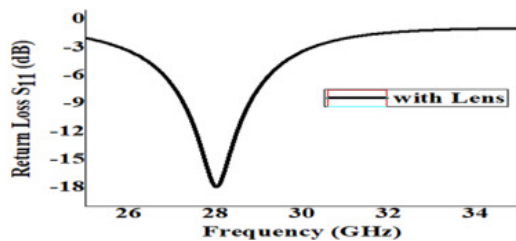


Fig. 14. Return loss ( $S_{11}$ ) of the proposed antenna design with lens.

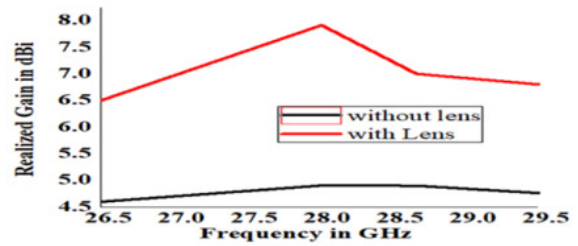


Fig. 15. Comparison of the realized gain of the proposed antenna design with and without lens.

D. Comparison with Previous Studies

Table II compares the current study's results with the reported structures in the literature.

TABLE II. COMPARISON WITH PREVIOUS STUDIES

Reference	Method	Frequency (GHz)	Gain (dBi)	Proposed antenna (mm <sup>3</sup> )
[4]	H-shaped resonator	2.3–3.9	7.4	80×70×10.4
[6]	Multi layered SRR	5.6–7.8	10	75.5 ×37×5
[10]	FSS	7.6	7.22	64×64×35.2
[13]	lens with DRE's	6	16.7	210×210×230
[21]	Superstrate lens	5.8	10	52×52×28.4
[23]	MSPG method	17.1	16.5	130×130×41.5
[24]	MSPG method	28	12.4	50×50×20
This work	MS Luneburg lens	28	7.9	40 × 40 × 0.5

In terms of gain, the proposed antenna outperforms those presented in [4, 6], demonstrating a higher gain. However, while antennas in [6, 13, 21, 23, 24] offer greater gain than the introduced design, their larger dimensions make them impractical for 5G applications, where space efficiency is critical. Specifically, antennas in [6, 24] utilize multi-layered split-ring resonators and metasurfaces with phase gradient lenses to enhance gain, but the increased size of these components is a significant disadvantage.

The antenna and metasurface Luneburg lens proposed in this study are particularly suitable for 5G applications due to their compact nature. This single layer metasurface design not only provides effective gain enhancement at 28 GHz, but also maintains a small form factor, making it easily integrable with compact antenna designs. Unlike traditional methods that rely on complex fractal structures, multi-layer designs, and three-dimensional unit cells -approaches that increase complexity and space requirements- the proposed design offers a simpler, more efficient solution. Additionally, reducing the number of FSS layers and the distance between the antenna and the lens further improves compactness without sacrificing performance. While the use of FSS-based reflectors to boost the antenna gain is well-established, the distance between the antenna and the reflector plays a critical role in determining the peak gain. The proposed design successfully balances size, gain, and complexity, addressing key challenges in modern antenna design for 5G communication systems.

III. CONCLUSIONS

This paper presents the design of a compact, low-return-loss millimetre-wave antenna suitable for 5G applications. The proposed antenna operates at a frequency of 28 GHz and

utilizes a metasurface Luneburg lens, offering a simplified approach compared to traditional, more complex structures. The antenna is based on a quarter-wave transformer-coupled slotted rectangular microstrip patch, with dimensions of 3.29 mm in length and 4.23 mm in width, designed to resonate at the target frequency of 28 GHz. The metasurface Luneburg lens, consisting of two distinct unit cells, is integrated with the patch antenna to improve performance at the resonant frequency. This integration enhances critical parameters, such as the antenna gain and return loss. The simulation results reveal that the proposed antenna achieves a gain of 7.9 dBi and a return loss of less than -10 dB, with a compact dimension of 40 mm × 40 mm × 0.5 mm. Due to its small size, effective gain, and low return loss, the proposed antenna design holds promise as a viable solution for 5G communication systems, where compactness and performance are essential.

#### REFERENCES

- [1] H. A. Diawuo and Y.-B. Jung, "Broadband Proximity-Coupled Microstrip Planar Antenna Array for 5G Cellular Applications," *IEEE Antennas and Wireless Propagation Letters*, vol. 17, no. 7, pp. 1286–1290, Jul. 2018, <https://doi.org/10.1109/LAWP.2018.2842242>.
- [2] J. Zeng and K.-M. Luk, "Single-Layered Broadband Magnetolectric Dipole Antenna for New 5G Application," *IEEE Antennas and Wireless Propagation Letters*, vol. 18, no. 5, pp. 911–915, Feb. 2019, <https://doi.org/10.1109/LAWP.2019.2905768>.
- [3] V. P. Sarin, M. S. Nishamol, D. Tony, C. K. Aanandan, P. Mohanan, and K. Vasudevan, "A Broadband L-Strip Fed Printed Microstrip Antenna," *IEEE Transactions on Antennas and Propagation*, vol. 59, no. 1, pp. 281–284, Jan. 2011, <https://doi.org/10.1109/TAP.2010.2090641>.
- [4] H. Wang, S.-F. Liu, L. Chen, W.-T. Li, and X.-W. Shi, "Gain Enhancement for Broadband Vertical Planar Printed Antenna With H-Shaped Resonator Structures," *IEEE Transactions on Antennas and Propagation*, vol. 62, no. 8, pp. 4411–4415, Dec. 2014, <https://doi.org/10.1109/TAP.2014.2325955>.
- [5] A. Rivera-Albino and C. A. Balanis, "Gain Enhancement in Microstrip Patch Antennas Using Hybrid Substrates," *IEEE Antennas and Wireless Propagation Letters*, vol. 12, pp. 476–479, 2013, <https://doi.org/10.1109/LAWP.2013.2256333>.
- [6] A. Dadgarpour, A. A. Kishk, and T. A. Denidni, "Gain Enhancement of Planar Antenna Enabled by Array of Split-Ring Resonators," *IEEE Transactions on Antennas and Propagation*, vol. 64, no. 8, pp. 3682–3687, Dec. 2016, <https://doi.org/10.1109/TAP.2016.2565741>.
- [7] J. H. Kim, C.-H. Ahn, and J.-K. Bang, "Antenna Gain Enhancement Using a Holey Superstrate," *IEEE Transactions on Antennas and Propagation*, vol. 64, no. 3, pp. 1164–1167, Mar. 2016, <https://doi.org/10.1109/TAP.2016.2518650>.
- [8] H. Boutayeb and T. A. Denidni, "Gain Enhancement of a Microstrip Patch Antenna Using a Cylindrical Electromagnetic Crystal Substrate," *IEEE Transactions on Antennas and Propagation*, vol. 55, no. 11, pp. 3140–3145, Aug. 2007, <https://doi.org/10.1109/TAP.2007.908818>.
- [9] A. Swetha and K. Rama Naidu, "Gain enhancement of an UWB antenna based on a FSS reflector for broad band applications," *Progress In Electromagnetics Research C*, vol. 99, pp. 193–208, 2020, <https://doi.org/10.2528/PIERC19120905>.
- [10] S. Maity, T. Tewary, S. Mukherjee, A. Roy, P. P. Sarkar, and S. Bhunia, "Wideband hybrid microstrip patch antenna and gain improvement using frequency selective surface," *International Journal of Communication Systems*, vol. 35, no. 14, 2022, Art. no. e5268, <https://doi.org/10.1002/dac.5268>.
- [11] D. D. Nguyen and C. Seo, "A wideband high gain trapezoidal monopole antenna backed by frequency selective surface," *Microwave and Optical Technology Letters*, vol. 63, no. 9, pp. 2392–2399, 2021, <https://doi.org/10.1002/mop.32890>.
- [12] S. Rajasri and R. B. Rani, "CPW-fed octagonal-shaped metamaterial-inspired multiband antenna on frequency selective surface for gain enhancement," *Applied Physics A*, vol. 128, no. 7, Jun. 2022, Art. no. 594, <https://doi.org/10.1007/s00339-022-05742-3>.
- [13] Y. Chen, L. Chen, J.-F. Yu, and X.-W. Shi, "A C-Band Flat Lens Antenna With Double-Ring Slot Elements," *IEEE Antennas and Wireless Propagation Letters*, vol. 12, pp. 341–344, 2013, <https://doi.org/10.1109/LAWP.2013.2247973>.
- [14] A. Dhoubi, S. N. Burokur, A. de Lustrac, and A. Priou, "Compact Metamaterial-Based Substrate-Integrated Luneburg Lens Antenna," *IEEE Antennas and Wireless Propagation Letters*, vol. 11, pp. 1504–1507, 2012, <https://doi.org/10.1109/LAWP.2012.2233191>.
- [15] A. R. Weily and N. Nikolic, "Dual-Polarized Planar Feed for Low-Profile Hemispherical Luneburg Lens Antennas," *IEEE Transactions on Antennas and Propagation*, vol. 60, no. 1, pp. 402–407, Jan. 2012, <https://doi.org/10.1109/TAP.2011.2167941>.
- [16] Z. L. Mei, J. Bai, T. M. Niu, and T. J. Cui, "A Half Maxwell Fish-Eye Lens Antenna Based on Gradient-Index Metamaterials," *IEEE Transactions on Antennas and Propagation*, vol. 60, no. 1, pp. 398–401, Jan. 2012, <https://doi.org/10.1109/TAP.2011.2167914>.
- [17] Z. Tao, D. Bao, H. X. Xu, H. F. Ma, W. X. Jiang, and T. J. Cui, "A Millimeter-Wave System of Antenna Array and Metamaterial Lens," *IEEE Antennas and Wireless Propagation Letters*, vol. 15, pp. 370–373, 2016, <https://doi.org/10.1109/LAWP.2015.2446500>.
- [18] A. K. Singh, M. P. Abegaonkar, and S. K. Koul, "Wide Angle Beam Steerable High Gain Flat Top Beam Antenna Using Graded Index Metasurface Lens," *IEEE Transactions on Antennas and Propagation*, vol. 67, no. 10, pp. 6334–6343, Jul. 2019, <https://doi.org/10.1109/TAP.2019.2923075>.
- [19] Y.-X. Zhang, Y.-C. Jiao, and S.-B. Liu, "3-D-Printed Comb Mushroom-Like Dielectric Lens for Stable Gain Enhancement of Printed Log-Periodic Dipole Array," *IEEE Antennas and Wireless Propagation Letters*, vol. 17, no. 11, pp. 2099–2103, Aug. 2018, <https://doi.org/10.1109/LAWP.2018.2851298>.
- [20] Q. L. Li, S. W. Cheung, D. Wu, and T. I. Yuk, "Microwave Lens Using Periodic Dielectric Sheets for Antenna-Gain Enhancement," *IEEE Transactions on Antennas and Propagation*, vol. 65, no. 4, pp. 2068–2073, Apr. 2017, <https://doi.org/10.1109/TAP.2017.2670441>.
- [21] D.-N. Dang and C. Seo, "High Gain Antenna Miniaturization With Parasitic Lens," *IEEE Access*, vol. 8, pp. 127181–127189, 2020, <https://doi.org/10.1109/ACCESS.2020.3008234>.
- [22] H.-X. Xu, G.-M. Wang, Z. Tao, and T. Cai, "An Octave-Bandwidth Half Maxwell Fish-Eye Lens Antenna Using Three-Dimensional Gradient-Index Fractal Metamaterials," *IEEE Transactions on Antennas and Propagation*, vol. 62, no. 9, pp. 4823–4828, Sep. 2014, <https://doi.org/10.1109/TAP.2014.2330615>.
- [23] L. Hua *et al.*, "Bidirectional radiation high-gain antenna based on phase gradient metasurface," *Applied Physics B*, vol. 127, no. 9, Aug. 2021, Art. no. 136, <https://doi.org/10.1007/s00340-021-07684-9>.
- [24] P. Das and A. K. Singh, "Gain Enhancement of Millimeter Wave Antenna by Ultra-thin Radial Phase Gradient Metasurface for 5G Applications," *IETE Journal of Research*, vol. 70, no. 3, pp. 2400–2408, Mar. 2024, <https://doi.org/10.1080/03772063.2023.2191998>.
- [25] S. Budumuru, G. Allu, D. Jenjeti, V. S. A. Tanakala, and S. R. Sankranti, "Design of a Funnel-Shaped MIMO Antenna for RADAR Applications," *Engineering, Technology & Applied Science Research*, vol. 14, no. 5, pp. 16808–16812, Oct. 2024, <https://doi.org/10.48084/etasr.8177>.